Throughput Measurements and Capacity Estimates for Quantum Connections

Nageswara S. V. Rao, Muneer Alshowkan,
Joseph C. Chapman, and Nicholas A. Peters,
Oak Ridge National Laboratory
Oak Ridge, TN 37831, USA
{raons,alshowkanm,chapmanjc,petersna}@ornl.gov

Joseph M. Lukens
Arizona State University
Phoenix, AZ 85004, USA
joseph.lukens@asu.edu

***Abstract*—The throughput of conventional and quantum network connections is an important performance metric typically specified by bps and ebps, respectively. It is measured in practical quantum network connections using specialized methods, and estimated using analytical bounds for which extensive theory has been developed. For practical connections, however, these two quantities have often been hard to correlate due to the lack of measurements and estimates derived under well-characterized common conditions. They both differ significantly from the conventional network throughput of TCP which employs buffers and loss recovery mechanisms. We describe a conventional-quantum testbed that enables the comparison of these two quantities both qualitatively and quantitatively. The conventional and quantum network throughput is measured over fiber connections of lengths over 75 kilometers, which show that the former decreases significantly slower with distance than the latter and in a qualitatively different way. The analytic capacity estimates of ebps are derived using approximations based on light intensity measurements which show a more rapid decrease with distance than the measured ebps throughput. These results provide qualitative insights into the conventional transport mechanisms based on buffers, and the conditions used in deriving analytical ebps capacity estimates.**

***Index Terms*—throughput estimates, capacity estimates, quantum-conventional network testbed**

I. Introduction

The throughput is a critical performance metric for connections in conventional and quantum networks. In conventional networks, it is typically measured as bits per second (bps). It has been extensively studied both analytically and experimentally [1], and is used in practice in the design and optimization of network infrastructures and protocols [2]. In quantum networks, there exist several candidate throughput performance metrics, based on quantities such as quantum bits (qubits), entangled bits (ebits), and secret-key bits (kbits). Among them, ebits per second (ebps) is particularly useful in characterizing the entanglement distribution performance, in particular, as a component of the teleportation throughput [3]. In this paper, we consider bps and ebps measurements collected over fiber connections, and analytical capacity estimates for ebps, all over repeater-less optical connections [4].

This manuscript has been co-authored by UT-Battelle, LLC, under contract DE-AC05-00OR22725 with the US Department of Energy (DOE). The US government retains and the publisher, by accepting the article for publication, acknowledges that the US government retains a nonexclusive, paid-up, irrevocable, worldwide license to publish or reproduce the published form of this manuscript, or allow others to do so, for US government purposes. DOE will provide public access to these results of federally sponsored research in accordance with the DOE Public Access Plan (http://energy.gov/downloads/doe-public-access-plan).

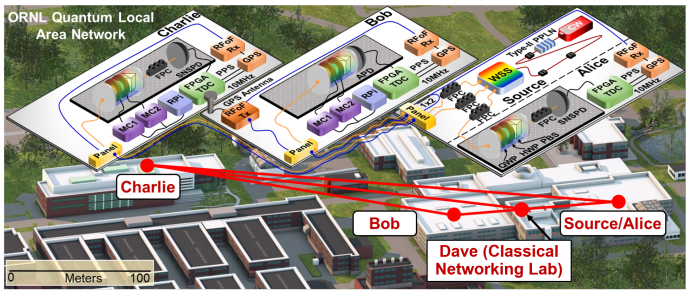

Fig. 1: Map of QNET on ORNL campus with three quantum nodes named Alice, Bob and Charlie, and a classical networking node named Dave. The quantum node configurations are shown as insets. The acronyms and labels are described in Table I.

The throughput in both cases depends on the connection length in addition to various other factors such as fiber material and quality, source quality and intensity, performance of detectors, and others. We mainly consider the effects of the connection length while keeping other parts nearly fixed. The conventional network throughput is measured using *iperf3* tool between host systems. In quantum networks, the ebps measurements require specialized equipment, for example, entanglement sources and Super-conducting Nanowire Single Photon Detectors (SNSPD) [5]. Extensive theory has been developed to estimate the capacity of quantum connections, which are modeled as generic quantum channels [3] and specialized for fiber connections by using the transmissivity as a key parameter [4]. They provide upper bounds on the achievable throughput which also provide qualitative information on the throughput decrease as a function of the connection length. In practice, however, ebps measurements and capacity estimates often are hard to correlate in part due to the lack of measurement platforms with precise, well-characterized analytic models.

In this paper, we describe a conventional-quantum testbed that provides measurements to support a comparison of these

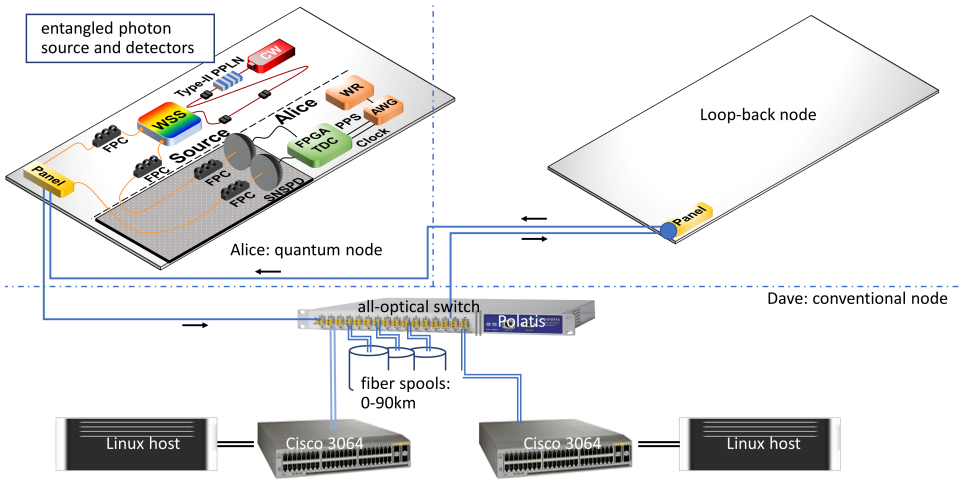

Fig. 2: QNET at ORNL augmented with fiber spools is used to provide connections of various lengths in a telescopic design for both conventional and quantum connections. The node Dave [5] utilizes all-optical Polatis switch to provide classical connections between pairs of switches and hosts and also optical cross-connects connecting fibers from quantum nodes Alice and Bob. The acronyms and labels are described in Table I.

two quantities both qualitatively and quantitatively, in addition to bps measurements. We collect ebps measurements over fiber connections of different lengths, and estimate the corresponding capacities using the light intensity measurements to approximate the transmissivity parameter. We augment the quantum network (QNET) [5] at the Department of Energy's Oak Ridge National Laboratory (ORNL) shown in Fig. 1 with fiber spools to provide a suite of single-mode fiber connections 0–90 km in length. We also measure the light intensities for these connections and use them in the analytical formulae in [4] to derive the corresponding ebps capacity estimates.

We compare bps and ebps measurements and the capacity estimates corresponding to the latter.

- For conventional connections, 10 Gbps peak throughput is achieved over most 0–90 km distances, as a result of the buffers and loss detection and retransmission mechanism of the Transmission Control Protocol (TCP) [1], which are not (commonly) used in ebps measurements and analytical capacity estimates.
- For quantum connections, ebps throughput decays sharply with distance, specifically faster than linear, compared to bps but slower than the capacity estimates derived using the light intensity measurements. Consequently, the ebps throughput is higher than the estimated capacity, which indicates a mismatch between the analytical model and physical connection properties.

Overall, this comparison highlights the critical differences between the underlying mechanisms and the potential for achieving higher ebps possibly by using TCP-like mechanisms.

The organization of this paper is as follows. The augmentation to QNET testbed [5] and the configurations used for measurements are described in Section II. The light intensity and bps measurements are described in Sections III-A and III-B, respectively, and the ebps measurements are described in Section III-C. The capacity estimates are described in Section IV, and they are compared with measurements in Section V. The conclusions and future directions are described in Section VI.

APD	avalanche photodiode
AWG	arbitrary waveform generator
CW	continuous-wave laser
FPC	fiber polarization controller
FPGA	field-programmable gate array
GPS	Global Positioning System
Panel	fiber-optic patch panel
PPLN	periodically poled lithium niobate
PPS	pulse per second
Source	entanglement source
SNSPD	superconducting nanowire single-photon detector
WR	White Rabbit clock system
WSS	wavelength-selective switch

TABLE I: Acronyms and labels of devices deployed in QNET using naming convention in [6].

II. QNET Testbed With Fiber Spool Telescoping

The QNET testbed [5]–[7], shown in Fig. 1, is augmented with six fiber spools to provide a set of connections for measuring the throughput along with the corresponding light intensity levels. The quantum node Alice and the conventional node Dave, shown in Fig. 2, are utilized in collecting ebps measurements. The quantum entanglement source and SNSPD are located at node Alice, and the quantum connections are routed through nodes Bob and Dave; the fiber is patched at the panel at node Bob and is connected via all-optical (Polatis) switch at node Dave by including fiber spools. Both ends of

Fig. 3: QNET conventional node Dave consists of two supermicro Linux hosts, two Cisco 3064 switches and a Polatis all-optical switch.

each fiber spool are connected to Polatis switch and can be cross-connected with others spools and fiber connections to nodes Alice and Bob. At node Dave, two conventional Ethernet switches (Cisco 3064), two hosts (Supermicro with 32 Intel CPUs) are connected to all-optical switch, as shown in Fig. 3.

The augmented fiber spools consist of three 25-km, one 10-km, one 5-km, and twelve 30-m single-mode fibers attached to all-optical switch. In our experiments, they are configured in a telescoping scheme by using them in combinations and switching on all-optical switch to provide the distances of 30 m and 5, 10, 15, 25, 30, 35, 40, 50, 55, 60, 65, 75, 80 and 90 km. These connections are provisioned and used one at a time as a part of either a conventional or quantum connection. The ends of such a fiber connection are connected to all-optical switch which provides the power levels at both ends and their difference is an estimate of the connection loss. These two ends are also cross-connected on all-optical switch to two Cisco switches, respectively, to form a conventional connection; they are cross-connected to fiber connections to nodes Alice and Bob to form a quantum connection, as shown in Fig. 2.

A conventional connection is established between two hosts connected to respective Cisco switches via 10Gbps 850nm multi-mode SFPs (Fig. 3). The Cisco switches are connected to all-optical switch via single mode fiber using two types of XFPs, 1310nm designed for site connections with 10km target distance, and 1550nm designed for 80km target distance. The bps measurements are collected using iperf3 running on the hosts with BBR TCP congestion control module.

Single-mode fiber connections from Alice to all-optical switch are used to test various-length quantum connections. This path consists of fiber connection from Alice to Bob to all-optical switch then back to Alice via different fiber path. Following the experimental design in [5], [7], the entangled photon source at Alice is composed of a 10-mm-long, periodically poled lithium niobate (PPLN) waveguide (HC Photonics), engineered for type-II spontaneous parametric down-conversion (SPDC). The entanglement distribution starts from the source in the quantum lab at node Alice. While

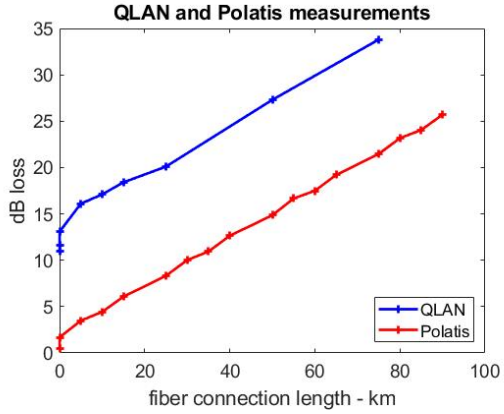

(a) Connection loss estimates

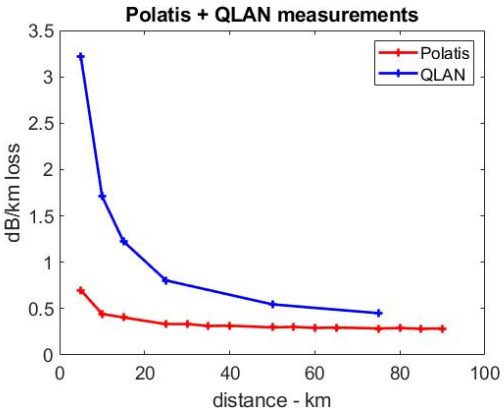

(b) loss per mile estimates

Fig. 4: Light level measurements are collected on all-optical Polatis switch, and at QNET source and detectors at node Alice, which are used in approximate capacity estimates: (a) connection losses based based on light intensity measurements are shown using Polatis and QNET measurements, and (b) losses per mile are estimated based on light level measurements.

one photon remains at Alice, the other is sent to the all-optical switch through several fiber spools, sent to Bob patch panel, then looped back to Alice for coincidence detection using SNSPDs (Quantum Opus). Components of the analyzer include a quarter-wave plate (QWP), half-wave plate (HWP), and polarizing beam splitter (PBS) outputs are directed to SNSPDs for coincidence measurement. After the polarization analyzers, the detectors are preceded by fiber polarization controllers (FPCs) to maximize the polarization-dependent detection efficiency.

In addition to the losses is fiber spools, there are about 15–20 dB total additional losses on the quantum connection (source through detection). There are losses on each side for source collection and detection efficiency and propagation from the quantum nodes to conventional node and back. The power level measurements are collected both at node Alice and on all-optical switch at node Dave for each quantum

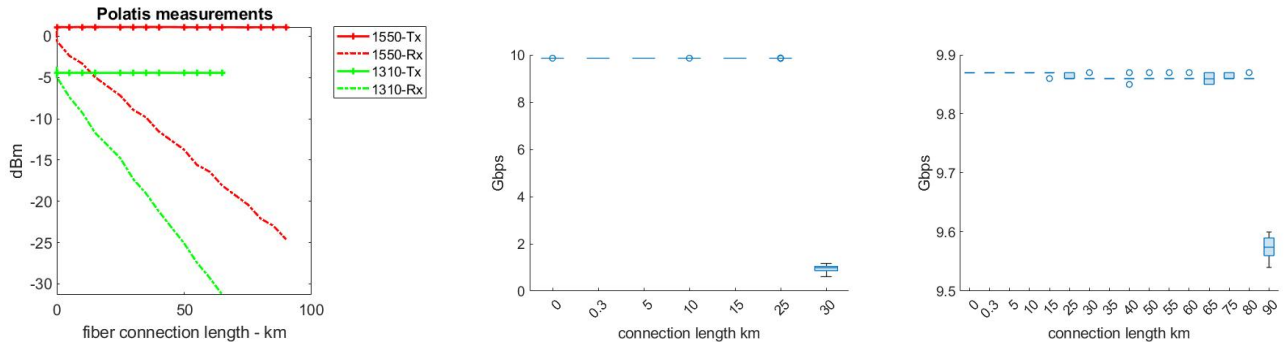

(a) transmit and receive powers (b) bps using 1310nm XFP (c) bps using 1550nm XFP

Fig. 5: Conventional throughput measurements: (a) Tx and Rx power levels, (b) bps using 1310nm LR 10Gbps XFP, (c) bps using 1550nm ER 10Gbps XFP.

connection.

III. Measurements Collection

The throughput measurements and the corresponding capacity estimates based on light level measurements provide complementary information about the achievable rates over the deployed quantum networks. The general expectation is that ebps measurements are below the capacity estimates which represent the maximum achievable throughput. In addition, the corresponding conventional throughput provides insights into the effects of TCP mechanisms of buffers and loss detection and recovery.

A. Light-level Measurements

For each conventional and quantum connection, the light levels (dBm) are measured on the all-optical switch, and these are referred to as Polatis measurements. For quantum connections, additional light level measurements are collected at the source and detectors in node Alice, and these are referred to as QNET measurements. The connection dB loss values obtained by subtracting destination levels from source levels are shown for both connections in Fig. 4(a) as a function of the connection length in km, which show a nearly linear trend. There is a nearly constant additional 15–20 dB loss for the quantum connections due to the additional fiber connections between nodes Alice and Dave, both direct and via node Bob, and at source and detectors. The loss rate per mile is estimated by dividing the connection losses by the connection length, and these estimates show a decreasing trend as the connection length is increased, as shown in Fig. 4(b). The higher values at shorter connections are due to the higher fraction of losses due to fiber patches at the nodes, cross-connects on all-optical switch and connections at the source and detectors. The transmit (Tx) and receive (Rx) light levels of 1310nm and 1550nm XFPs measured on Polatis switch are shown in Fig. 5(a); the former has lower Tx level due to its shorter target distance of 10km and its Rx levels decrease more rapidly due to its shorter wavelength.

B. Conventional Throughput Measurements

The bps measurements are collected using iperf3 between two Linux hosts at Dave connected through the all-optical switch. Using 1310 nm XFP, 10 Gbps throughput is achieved over 10 km but drops abruptly to $\sim$1 Gps at 30 km, as shown in Fig. 5(b). It is result in rapid drop in light levels on 30km connection, beyond which the light levels are not sufficient to establish TCP connection. This XFP achieves nearly 10Gbps for connections up to 25km in length, much larger than 10km in its specification. Using 1550 nm XFP, nearly 9.9 Gbps throughput is maintained over 80 km connections and reduces to about 9.6 Gbps at 90 km, as shown in Fig. 5(c). This XFP uses much higher source power measured 1.5-2.5 dBm. In both cases, the shape of the throughput profile is concave, which is typically observed in optimized conventional networks. On the other hand, performance bottlenecks such as insufficient TCP or other buffers would lead to a convex shape [2], which is observed both for ebps measurements shown in Fig. 6(a) and also their capacity estimates shown in Fig. 6(c). The Shannon capacity estimates for bps based on signal-to-noise ratio [8] are qualitatively similar to these capacity estimates, and they also have a convex shape since they do not include effects of buffers and loss recovery mechanisms.

C. Ebit Measurements

We measure the coincidence rates of our entangled photon source at various distances for Alice's channel and calculate the entanglement throughput by assuming the quantum state fidelity is 1, which is a good assumption since our state fidelity is $> 90\%$ for these tests [7]. These measurements decrease with the connection length as shown in Fig. 6(a), and the profile is convex in sharp contrast with that of bps measurements. The corresponding connection losses are shown in Fig. 6(b) between the source and detectors at node Alice and the respective values on Polatis that correspond to fiber spools; the dB losses are nearly linear with respect to connection length with mean offset of 12.22 dB with standard deviation 0.46 dB. Indeed, TCP mechanisms of bps measurements lead to a more predictable and concave profile

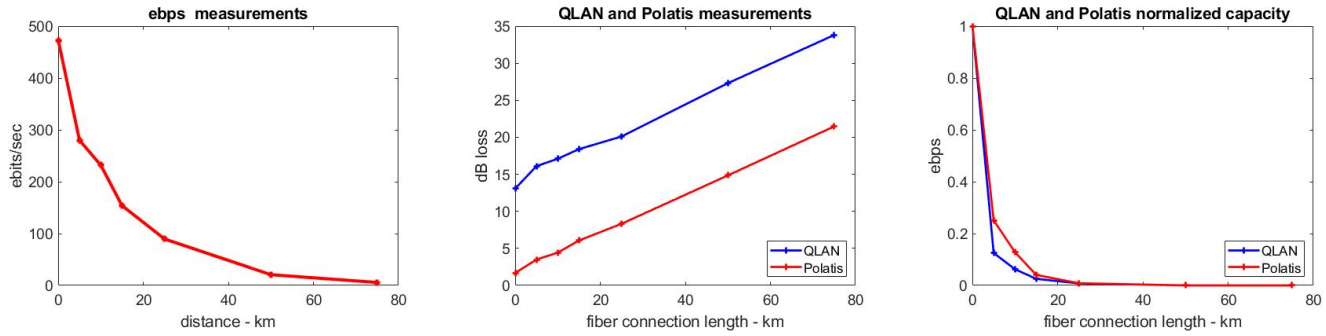

(a) ebps measurements (b) dB losses on QNET and Polatis (c) capacity estimates: QNET and Polatis

Fig. 6: Measurements of ebps collected over quantum connections and capacity estimates based on light levels have a convex profile with respect to the connection length. (a) epbs measurements, (b) connection dB losses, and (c) capacity estimates using light levels to derive approximate transmissivity estimates.

which decreases slower than a linear profile compared to the opposite of the ebps convex profile.

IV. Capacity Estimates based on Light Level Measurements

Capacity estimates for fiber connections are derived under various conditions using a variety of parameters, and also by specializing the general quantum channels specified by mathematical descriptions [3]. A generic quantum communications channel is defined as a linear, completely positive, trace preserving map, corresponding to a quantum physical evolution, and it takes a particular form according to a Choi–Kraus decomposition in terms of Kraus operators. Several versions of the quantum capacity are defined and estimated under various parametrizations, for example, dephasing and depolarizing [9]. Such channels models may be inferred by process tomography using measurements collected on QNET [9]. We consider a specific characterization based on simplified optical fiber channels without repeaters which uses the transmissivity parameter [4].

For fiber connections, we utilize the ebps capacity estimate per channel use derived based on the transmissivity η of the optical fiber derived in [4]

$$D_2(\eta) = -\log_2(1-\eta).$$

It provides a bound on ebits for channel use, which in turn corresponds to the channel rate when the source rate is fixed. Here, η is typically a linear function of the connection length, and consequently, the capacity profile is typically convex. The transmissivity in this case is defined as a fraction of entangled photons that are successfully transmitted through the connection, which we approximate as a fraction of the light level that passed through by converting the dB loss into fraction and subtracting from 1. This use of the connection light level transmission to approximate the transmissivity η involves the following approximations:

- QNET measurements utilize spectral filtering and calibration for 1560-nm entangled photons, and represent a bulk quantity that includes singles and entangled photons. The assumption is that the losses are not selective to either, and are representative of the entangled ones.
- Polatis measurements correspond to a broader spectrum than those in QNET measurements and have a coarser resolution with no spectral filtering and calibration. The assumption is that these losses are somewhat uniform around the frequency of entangled photons.
- The fiber connections consist of multiple cross-connects at the patch panel between the nodes, connections to and within Polatis switch. The capacity estimates are derived mainly using "pure" fiber models. These connections incur additional losses that effect both throughput measurements and light levels, and the assumption is that they play a secondary role particularly at longer connection lengths.

This estimation is approximate since the measured light level includes other components, particularly on the all-optical switch where no spectral filtering and calibration are performed. Using these values, we approximate η in both cases and compute the corresponding $D_2(\eta)$. The second estimate based on Polatis measurements corresponds to a shorter connection made up of only fiber spools, whereas the former includes connection between quantum and conventional nodes. The difference between them is evident in lower capacity estimate of the longer connections as shown in Fig. 6(c). The capacity estimates are derived mainly by treating the connections as entirely composed of fiber in [4] without explicitly accounting for patching and switching.

V. Measurements and Capacity Estimates

The ebps measurements and capacity estimates based on QNET measurements are normalized with the highest values over 30-m fiber spool connection; additionally, for illustration those based on Polatis measurements are also estimated which correspond to smaller connection losses by about 12.22 dB. Both ebps measurements and the corresponding capacity estimates decrease rapidly with distance in Fig. 7 as expected; in particular, the shape is convex which is similar to a TCP profile

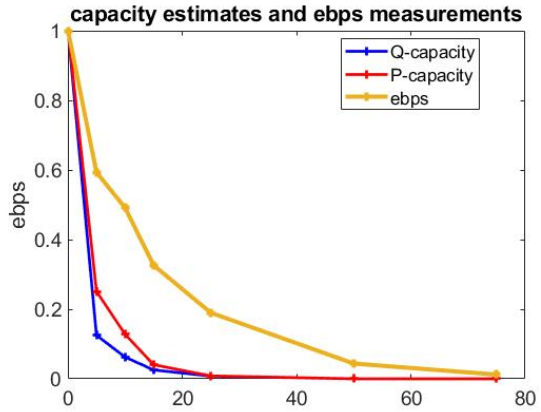

(a) Connection loss estimates

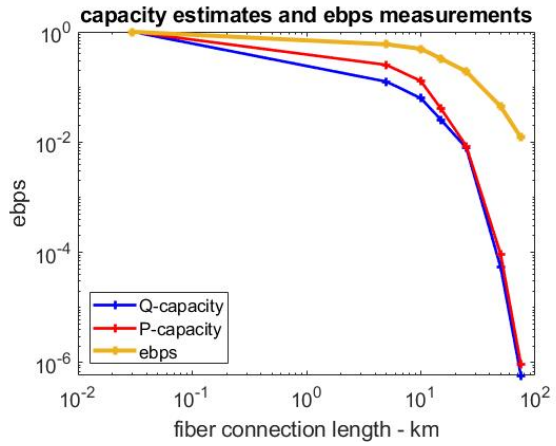

(b) Connection loss estimates

Fig. 7: The ebps measurements decrease slower than capacity estimates based on light level measurements. (a) ebps measurements and capacity estimates in original scale, and (b) ebps measurements and capacity estimates log-log scale.

under severe bottlenecks. While both decrease rapidly, the ebps measurements are higher than the capacity estimates as shown in Fig. 7. We postulate a certain degree of misalignment between the assumptions used for the capacity estimation and QNET conditions under which the light intensity measurements are collected. Situation is somewhat similar to Shannon limit [8] wherein several refinements were needed to correlate measurements with theoretical estimates.

VI. Conclusions

This work is an initial attempt to relate physical ebps measurements and the analytical estimates of throughput of quantum connections, and both to conventional network throughput that has been extensively studied both analytically and experimentally. We augmented QNET testbed with fiber spools to provision a suite of optical connections that enabled us to measure bps and ebps throughput and light levels used in ebps capacity estimates. Our results provided useful insights: (a) ebps throughput measurements exceed the capacity estimates based on light levels, which points to a mismatch between the experimental and analytic conditions, and (b) the throughput profiles of ebps and its capacity estimates are convex as a function of connection length, namely, they decay faster than linear, which is in sharp contrast concave profiles of TCP bps measurements that decrease slower than linear.

Overall, this study indicates the need for further investigation in several directions and the need for refinements in both measurements and analytical estimates. The approximation process using light levels could be potentially improved by refined analysis and measurements. Also, it highlights an open question on the role of buffers and loss recovery in sustaining ebps throughput, similar to TCP mechanisms in conventional networks.

VII. Acknowledgments

This research was performed in part at Oak Ridge National Laboratory, managed by UT-Battelle, LLC, for the U.S. Department of Energy under contract no. DE-AC05-00OR22725. U.S. Department of Energy, Office of Science, Advanced Scientific Computing Research, under the Entanglement Management and Control in Transparent Optical Quantum Networks and Early Career Research programs (Field Work Proposals ERKJ378 and ERKJ353).

References

[1] J. Schmid, A. Höss, and B. W. Schuller, "A survey on client throughput prediction algorithms in wired and wireless networks," *ACM Comput. Surv.*, vol. 54, oct 2021.

[2] N. S. V. Rao, Q. Liu, Z. Liu, R. Kettimuthu, and I. Foster, "Throughput analytics of data transfer infrastructures," in *Testbeds and Research Infrastructures for the Development of Networks and Communities* (H. Gao, Y. Yin, and H. Miao, eds.), 2019.

[3] M. M. Wilde. Cambridge University Press, 2 ed., Quantum Information Theory.

[4] S. Pirandola, R. Laurenza, C. Ottaviani, and L. Banchi, "Fundamental limits of repeaterless quantum communications," *Nature Communications*, vol. 8, pp. 15043 EP –, 2017.

[5] M. Alshowkan, P. G. Evans, B. P. Williams, N. S. V. Rao, C. E. Marvinney, Y.-Y. Pai, B. J. Lawrie, N. A. Peters, and J. M. Lukens, "Advanced architectures for high-performance quantum networking," *J. Opt. Commun. Netw.*, vol. 14, pp. 493–499, Jun 2022.

[6] M. Alshowkan, N. S. V. Rao, J. C. Chapman, B. P. Williams, P. G. Evans, R. C. Pooser, J. M. Lukens, and N. A. Peters, "Lessons learned on the interface between quantum and conventional networking," in *Driving Scientific and Engineering Discoveries Through the Integration of Experiment, Big Data, and Modeling and Simulation* (J. . Nichols, A. B. Maccabe, J. Nutaro, S. Pophale, P. Devineni, T. Ahearn, and B. Verastegui, eds.), (Cham), pp. 262–279, Springer International Publishing, 2022.

[7] M. Alshowkan, B. P. Williams, P. G. Evans, N. S. Rao, E. M. Simmerman, H.-H. Lu, N. B. Lingaraju, A. M. Weiner, C. E. Marvinney, Y.-Y. Pai, B. J. Lawrie, N. A. Peters, and J. M. Lukens, "Reconfigurable quantum local area network over deployed fiber," *PRX Quantum*, vol. 2, p. 040304, Oct 2021.

[8] M. Secondini and E. Forestieri, "The limits of the nonlinear shannon limit," in *2016 Optical Fiber Communications Conference and Exhibition (OFC)*, pp. 1–3, 2016.

[9] J. C. Chapman, J. M. Lukens, M. Alshowkan, N. Rao, B. T. Kirby, and N. A. Peters, "Coexistent quantum channel characterization using spectrally resolved bayesian quantum process tomography," 2022.